JOURNAL OF BACTERIOLOGY, Aug. 2009, p. 4996–5009 Vol. 191, No. 15
0021-9193/09/$08.00+0 doi:10.1128/JB.00307-09
Copyright © 2009, American Society for Microbiology. All Rights Reserved.

Identification of a Novel Self-Sufficient Styrene Monooxygenase from *Rhodococcus opacus* 1CP▽†

Dirk Tischler,[1]* Dirk Eulberg,[2]# Silvia Lakner,[2] Stefan R. Kaschabek,[1] Willem J. H. van Berkel,[3] and Michael Schlömann[1]

Environmental Microbiology, TU Bergakademie Freiberg, Leipziger Str. 29, 09596 Freiberg, Germany[1]; Department of Microbiology, University Stuttgart, Allmandring 31, 70569 Stuttgart, Germany[2]; and Laboratory of Biochemistry, Wageningen University, Dreijenlaan 3, 6703 HA Wageningen, The Netherlands[3]

Received 6 March 2009/Accepted 21 May 2009

Sequence analysis of a 9-kb genomic fragment of the actinobacterium *Rhodococcus opacus* 1CP led to identification of an open reading frame encoding a novel fusion protein, StyA2B, with a putative function in styrene metabolism via styrene oxide and phenylacetic acid. Gene cluster analysis indicated that the highly related fusion proteins of *Nocardia farcinica* IFM10152 and *Arthrobacter aurescens* TC1 are involved in a similar physiological process. Whereas 413 amino acids of the N terminus of StyA2B are highly similar to those of the oxygenases of two-component styrene monooxygenases (SMOs) from pseudomonads, the residual 160 amino acids of the C terminus show significant homology to the flavin reductases of these systems. Cloning and functional expression of His_{10}-StyA2B revealed for the first time that the fusion protein does in fact catalyze two separate reactions. Strictly NADH-dependent reduction of flavins and highly enantioselective oxygenation of styrene to (*S*)-styrene oxide were shown. Inhibition studies and photometric analysis of recombinant StyA2B indicated the absence of tightly bound heme and flavin cofactors in this self-sufficient monooxygenase. StyA2B oxygenates a spectrum of aromatic compounds similar to those of two-component SMOs. However, the specific activities of the flavin-reducing and styrene-oxidizing functions of StyA2B are one to two orders of magnitude lower than those of StyA/StyB from *Pseudomonas* sp. strain VLB120.

The incorporation of one atom of oxygen during hydroxylation, epoxidation, sulfoxidation, or Baeyer-Villiger oxidation is a common initial step of the aerobic degradation of aromatic compounds by microorganisms. In bacteria, these reactions are most frequently catalyzed by inducible flavoprotein monooxygenases (EC 1.14.13 [57]). The majority of these enzymes (so-called single-component flavoprotein monooxygenases) utilize electrons from NAD(P)H, which are transferred to a noncovalently bound flavin adenine dinucleotide (FAD) in order to activate molecular oxygen as a flavin (hydro)peroxide. Depending on the protonation of this intermediate and the type of substrate, an oxygen atom is then incorporated by nucleophilic or electrophilic attack. More recently, different two-component flavoprotein monooxygenases have been characterized (57). These systems cover an NAD(P)H-dependent flavin reductase in order to generate reduced flavin and an oxygenase that utilizes this cofactor for the activation of oxygen.

The exquisite regio- and stereoselectivities of oxygen insertion by flavoprotein monooxygenases favor these enzymes for biocatalytic applications (23, 24, 33). This is especially true because chemical synthesis approaches by hetero- or homogenic catalysis often do not yield a sufficiently high enantiomeric excess for the production of pharmaceuticals and their chiral building blocks. The use of oxygen as an inexpensive nontoxic oxidant and mild reaction conditions are additional advantages with the potential for increasing the environmental sustainability of oxygenase-catalyzed biotransformations.

The necessity for expensive cofactors is perhaps the most striking drawback limiting the industrial application of flavoprotein monooxygenases. Different electrochemical and enzymatic procedures for in vitro cofactor regeneration are available (20, 21, 32, 52, 56), but these systems are currently lacking long-term stability. As a consequence, the practical application of flavoprotein monooxygenases is virtually restricted to in vivo systems in which cofactor regeneration is mediated by the metabolism of the expression host (45, 49). The limitations of whole-cell-mediated biotransformations by substrate and/or product toxicity can be overcome by means of two-phase systems, as was recently shown for the two-component styrene monooxygenase (SMO) from *Pseudomonas* sp. strain VLB120 (45).

Two-component flavoprotein monooxygenases present additional challenges for biocatalytic applications. The need for two separate protein components may hamper attempts at recombinant enzyme expression, the application of immobilized enzymes in cell-free systems, and the detection of novel oxygenases during activity-based metagenome-screening approaches. Moreover, and as was already shown for the two-component SMO from *Pseudomonas* sp. strain VLB120 (44), the interprotein transfer of reduced FAD is accompanied to a certain extent by the auto-oxidative formation of reactive oxygen species such as hydrogen peroxide (Fig. 1). Auto-oxidation of reduced FAD not only decreases the efficiency of the

* Corresponding author. Mailing address: Environmental Microbiology, TU Bergakademie Freiberg, Leipziger Str. 29, 09596 Freiberg, Germany. Phone: 49-3731-393739. Fax: 49-3731-393012. E-mail: Dirk-Tischler@email.de.

Present address: NOXXON Pharma AG, Max-Dohrn-Str. 8-10, D-10589 Berlin, Germany.

† Supplemental material for this article may be found at http://jb.asm.org/.

▽ Published ahead of print on 29 May 2009.

Downloaded from jb.asm.org at Wageningen UR Library on August 23, 2009

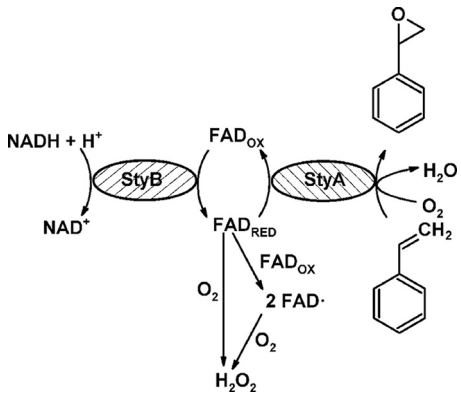

FIG. 1. Catalytic mechanism of two-component SMOs and the formation of oxidative stress by uncoupling between FAD oxidoreductase (StyB) and oxygenase (StyA) (adapted from reference 36). FAD_{OX} and FAD_{RED}, oxidized and reduced forms of FAD, respectively.

oxygenation process but also negatively interferes with the physiological conditions of the cell. The extent of oxidative stress is considerably increased when FAD oxidoreductase activity exceeds oxygenase activity and uncoupling becomes dominant.

Presently the details of reduced-FAD transfer between the oxygenase and FAD oxidoreductase components of SMOs are not known. Recent kinetic studies have indicated that reduced FAD is transferred by a mixed mechanism in which direct contact of both proteins and free diffusion of the reduced cofactor play a role (25). This hypothesis is supported by the work of Otto and coworkers in which the formation of hydrogen peroxide was shown to be reciprocally proportional to the concentration of active oxygenase StyA (44). The high level of efficiency of self-sufficient cytochrome P450 enzymes compared to that of multicomponent types is attributed to the closer location between the heme-containing P450 domain (oxygenase) and a reductase domain (FAD/flavin mononucleotide [FMN] and NADH binding site), which should also promote the efficiency of diffusive transfer (38). These self-sufficient P450 systems are of high biocatalytic interest (8, 34, 39), and it is likely that other types of self-sufficient monooxygenases (e.g., flavoenzymes) behave in a similar way.

Members of the gram-positive genus *Rhodococcus* are characterized by their exceptionally high level of metabolic versatility toward a broad range of organic substrates (31). Large genome sizes, the presence of megaplasmids, and a distinct gene redundancy (multiple enzyme homologs) favor these organisms as a promising source for novel enzymes (59). Moreover, several studies have provided evidence of functionally convergent evolution of the catabolic activities of rhodococci and proteobacteria (12, 37). Since most research on bacterial catabolic activities has so far been performed on the latter group, novel enzymes and mechanisms are likely to be identified in gram-positive bacteria.

The nocardioform actinobacterium *Rhodococcus opacus* 1CP was originally isolated from contaminated soil by enrichment with 4-chloro- and 2,4-dichlorophenol as the sole carbon sources (18). To solve questions related to the enzymes involved in chlorophenol mineralization, an *R. opacus* 1CP clone library was generated, leading to the identification of a 9-kb genomic fragment harboring genes with a presumed function in styrene metabolism. Sequence analysis indicated the presence of an open reading frame (ORF) encoding a fusion protein composed of an oxygenase and a reductase subunit with a high level of similarity to the corresponding subunits of two-component SMOs from pseudomonads. Recombinant expression and biochemical characterization confirmed that it has enantioselective styrene epoxidation ability and showed that StyA2B is the first representative of a new class of NADH- and flavin-dependent single-component flavoprotein monooxygenases.

MATERIALS AND METHODS

Chemicals and enzymes. Oxygenation substrates, (*S*)- and (*R*)-styrene oxide, and cofactors were purchased from Sigma-Aldrich (Steinheim, Germany) and Carl Roth (Karlsruhe, Germany). Enzymes used for cloning purposes were obtained from MBI Fermentas (St. Leon-Rot, Germany) and Roche Diagnostics. Oligonucleotides were synthesized by Eurofins MWG (Ebersberg, Germany). 4-Chlorostyrene oxide, 4-methylstyrene oxide, and dihydronaphthalene oxide were synthesized from the corresponding olefins (27).

Bacterial strains, plasmids, and culture conditions. The bacterial strains and plasmids used in this study are listed in Table 1. *R. opacus* 1CP was kept on mineral medium plates (9) with 54 mM sodium-potassium phosphate (pH 7.3) containing 5 mM benzoate at 30°C. Fed batch cultivation on styrene was performed in baffled 1-liter shaking flasks filled with 100 ml of the above mineral medium (30°C; 120 rpm). In total, 60 to 120 μl of styrene, corresponding to a total substrate load of 5 to 10 mM, was added in 2.5- to 15-μl portions over several days by means of an evaporation adapter. *Escherichia coli* strains were cultivated as described previously (50).

GC-MS-based metabolite detection during growth of *R. opacus* 1CP on styrene. The clear supernatant (20 min; 16,000 × *g*; 4°C) from 5 ml of an actively growing styrene culture (optical density at 600 nm [OD_{600}], ~0.3 to 1.5) was subjected to immersion solid phase microextraction (polydimethylsiloxane/divinylbenzene phase) (Supelco). After desorption, analytes were separated by two-dimensional gas chromatography (GC) (7890A GC system; Agilent) with RTX-5 (10 m; Restek) and RTX-17 (1.2 m; Restek) columns, using the following temperatures: 40°C (1 min), 40 to 60°C (plus 10°C min^{-1}), 60 to 100°C (plus 4°C min^{-1}), 100°C (1 min), and 100 to 250°C (plus 15°C min^{-1}). Spectra were detected using time-of-flight mass spectrometry (MS) (Pegasus 4D GCxGC-TOFMS; Leco) with an ionization field of −70 eV and a detector voltage of 1,450.

DNA techniques and purification of nucleic acids. Genomic DNA from *R. opacus* 1CP was prepared as described previously (37), and standard protocols were used for DNA cloning, transformation, and nucleic acid purification (22, 50).

Construction and functional screening of a clone library. Genomic 1CP DNA was partially digested with Sau3AI to get 3- to 6-kb fragments. Ligation in BamHI-digested dephosphorylated pBluescript II KS(+) and transformation into *E. coli* DH5α yielded a clone library. Transformants were plated onto LB agar (100 μg ml^{-1} ampicillin) and incubated at 37°C for 24 h. Following a 1-week incubation at 4°C, grown colonies were screened for blue coloration.

Restriction analysis, subcloning, and DNA sequencing of p1CPS1 and p1CPS2. Subclones of pBluescript II KS(+) p1CPS1 and pBluescript II KS(+) p1CPS2 were generated using restriction endonucleases ApaI, BamHI, EcoRI (only for p1CPS1), PstI, SacI, SacII, SmaI (only for p1CPS2), and XhoI. DNA sequencing was performed according to a dye terminator sequencing cycle protocol (54) and using Lasergene 99 program package v4.05 (Dnastar) and BLAST (2, 3) for sequence analysis.

Localization of overlapping clone p1CPS2 by hybridization. Digoxigenin (DIG) labeling, blotting, hybridization, and detection procedures were performed as described previously (29). A 688-bp BamHI/SpeI fragment of plasmid p1CPS1 served as a template for probe preparation, and genomic 1CP DNA was digested with the endonucleases ApaI, BamHI, EcoRI, and PstI.

Construction of expression clones for StyA1 and StyA2B. Genes *styA2B* and *styA1* were amplified from genomic 1CP DNA by PCR (annealing temperature, 61°C), using the appropriate primers (Table 1). Purified products of correct size (*styA2B*, 1,722 bp; *styA1*, 1,221 bp) were cloned into a T vector of pBluescript II KS(+) (35) and pJET1.2/blunt to yield pSRoA2B_B01 and pSRoA1_B01, respectively. Following double digestion by NdeI/NotI, *styA2B* and *styA1* were transferred in pET16bP to yield expression constructs pSRoA2B_P01 and

Downloaded from jb.asm.org at Wageningen UR Library on August 23, 2009

TABLE 1. Strains, plasmids, and primers used in this study

Strain, plasmid, or primer	Relevant characteristic(s)[a]	Source or reference(s)
Strains		
R. opacus 1CP	Benzoate$^+$, 4-hydroxybenzoate$^+$, 3-chlorobenzoate$^+$, phenol$^+$, 4-chlorophenol$^+$, 2,4-dichlorophenol$^+$, 2-chlorophenol$^+$, 3-methylphenol$^+$, 4-methylphenol$^+$, phthalate$^+$, isophthalate$^+$, *n*-alkanes$^+$ (C_{10}-C_{16}), and styrene^{+b}	18, 37
E. coli DH5α	F^- ϕ80d*lacZ*M15 (*lacZYA-argF*)*U169 endA1 recA1 hsdR17*(r_K^- m_K^+) *supE44* λ^- *thi-1 gyrA96 relA1*	Gibco-BRL
E. coli BL21(DE3) (pLysS)	*hsdS gal* (λc*Its*857 *ind*1 Sam7 *nin*5 *lacUV5*-T7 gene 1) pLysS (Cm^r)	Stratagene
Plasmids		
pBluescript II KS(+)	Phagemid derived from pUC19; P_{lac} *lacZ′* Ap^r; f1(+) origin; ColE1 origin	Stratagene
pJET1.2/blunt	Contains a gene coding for a lethal restriction enzyme; a gene disrupted by ligation of a DNA insert into the cloning site is possible; T7 promoter	Fermentas
pET16bP	pET16b with additional multicloning site; allows expression of recombinant proteins with N-terminal His_{10} tag	U. Wehmeyer[c]
p1CPS1	5,542-kb Sau3AI fragment of genomic *R. opacus* 1CP DNA in pBluescript II KS(+)	This study
p1CPS2	4,850-kb EcoRI fragment of genomic *R. opacus* 1CP DNA in pBluescript II KS(+)	This study
pSRoA2B_B01	*styA2B* of *R. opacus* 1CP (PCR product with primers 1CP_A2B_fw/1CP_A2B_rev) cloned into the EcoRV site of pBluescript II KS(+)	This study
pSRoA2B_P01	*styA2B* of *R. opacus* 1CP (1.722-kb NdeI/NotI fragment) cloned into pET16bP	This study
pSRoA1_B01	*styA1* of *R. opacus* 1CP (PCR product with primers 1CP_A1_fw/1CP_A1_rev) cloned into pJET1.2/blunt	This study
pSRoA1_P01	*styA1* of *R. opacus* 1CP (1.221-kb NdeI/NotI fragment) cloned into pET16bP	This study
Primers		
1CP_A1_fw	5′-CATATGCGCAAGATCACCATCGTT-3′; includes NdeI site	This study
1CP_A1_rev	5′-GCGGCCGCGAGTGCTAGTTC-3′; includes NotI site	This study
1CP_A2B_fw	5′-CATATGCGCAGCATCGCTAT-3′; includes NdeI site	This study
1CP_A2B_rev	5′-GCGGCCGCTCAGAAGTCG-3′; includes NotI site	This study
T3	5′-CGCGCAATTAACCCTCACTAAAG-3′; IRD800 labeled	Eurofins MWG
T7	5′-GCGCGTAATACGACTCACTATAG-3′; IRD800 labeled	Eurofins MWG

[a] Underlined primer regions indicate corresponding gene sequences.
[b] Plus signs indicate growth substrates.
[c] Personal communication.

pSRoA1_P01, from which recombinant proteins were obtained as His_{10}-tagged fusion proteins.

Expression, purification, and proteolytic cleavage of His_{10}-StyA2B. Recombinant expression took place in a 5-liter biofermenter (ADI 1030 biocontroller; Applikon). For that purpose, *E. coli* BL21(pSRoA2B_P01) was cultivated in 4 liters of LB medium (100 μg ml^{-1} ampicillin and 35 μg ml^{-1} chloramphenicol) at 30°C (600 rpm; 0.3 standard liters of air per minute) to an OD_{600} of 0.7. The addition of 0.1 mM IPTG (isopropyl-β-D-thiogalactopyranoside) was followed by an induction period of 27 h at 20°C. Cells were harvested by centrifugation, resuspended in 27 mM sodium-potassium phosphate (pH 7.3), and stored at −80°C.

Crude extract was prepared from the freshly thawed biomass after it was diluted with a threefold excess of 10 mM Tris HCl (pH 7.5) containing 2 mM dithiothreitol (DTT) as described previously (54).

Purification of His_{10}-StyA2B was achieved by Ni chelate chromatography on a 1-ml HisTrap FF column, using an ÄKTA fast-performance liquid chromatographer (both from GE Healthcare). After the application of a crude extract of *E. coli* BL21(pSRoA2B_P01) (290 mg total protein), nonspecific proteins were removed with binding buffer (10 mM Tris HCl [pH 7.5], 2 mM DTT, 0.5 M NaCl, 25 mM imidazole). His_{10}-StyA2B was eluted with a linear imidazole gradient of 25 to 500 mM in that buffer over 10 column volumes. Fractions with NADH-dependent FAD oxidoreductase activity were pooled and subjected to ammonium sulfate precipitation (80% saturation). Recombinant protein was collected by centrifugation, washed two times with 10 mM Tris HCl (pH 7.3) containing 4 M ammonium sulfate and 0.5 mM disodium EDTA, dissolved in storage buffer (100 mM Tris HCl [pH 7.25] containing 50% [vol/vol] glycerol, 5 mM DTT, and 100 mM ammonium sulfate) to a final concentration of 16 mg ml^{-1}, and stored at −20°C.

Attempts to express His_{10}-StyA1 by means of *E. coli* BL21(pSRoA1_P01) were restricted to 50-ml cultures in shaking flasks, since all conditions tested (0.1 to 1.0 mM IPTG; 20 to 30°C induction temperature) led exclusively to inactive inclusion bodies.

Estimation of molecular size of His_{10}-StyA2B. Discontinuous sodium dodecyl sulfate-polyacrylamide gel electrophoresis (SDS-PAGE) (50) and size exclusion chromatography on a Superdex 200 HR 16/60 column (GE Healthcare) were applied in order to determine the molecular sizes of denatured and native enzymes, respectively. For the latter technique, 100 mM Tris HCl (pH 7.5) containing 150 mM NaCl served as the mobile phase and low- and high-molecular-weight reference proteins (Amersham Pharmacia) were used for size calibration.

Protein determination and flavin and metal content analysis. Protein concentrations were determined with the Bradford method (6), using protein assay reagent (Bio-Rad). Bovine serum albumin (Sigma) served as the reference protein. His_{10}-StyA2B concentrations in small sample volumes were alternatively determined at 280 nm, using a NanoDrop photometer (Peqlab).

The flavin content of homogeneous His_{10}-StyA2B was determined spectrophotometrically by applying a molecular absorption coefficient of ε450 nm = 11.3 mM^{-1} cm^{-1} for free FAD (46). The metal content of a solution of 0.65 mg ml^{-1} His_{10}-StyA2B in 1% ultrapure HNO_3 was analyzed by inductively coupled plasma-atom emission spectroscopy using an iCAP 6500 instrument (Thermo Fisher Scientific) and compared to data obtained from a blank probe without protein.

SMO activity assays and inhibition studies. StyA2B activity was determined with respect to reduced flavin components at the expense of NAD(P)H as well as its ability to convert styrene or related substrates to the corresponding oxides.

Flavin oxidoreductase activity was measured spectrophotometrically following NADH consumption at 340 nm (Cary 50; Varian). The standard assay contained the following in a final volume of 1 ml: 20 μmol Tris HCl (pH 7.5), 0.175 μmol NADH, 0.050 μmol FAD, and an appropriate amount of recombinant StyA2B. After 10 min of preincubation at 30°C, the reaction was started by adding NADH. In order to determine enzyme specificity, NADPH, FMN, and riboflavin were applied as alternative cosubstrates. Initial reaction rates were measured using 4 to 60 μM flavin-containing electron acceptor and 17.5 to 175 μM NADH. Kinetic parameters (K_m and V_{max}) were obtained by the nonlinear least-squares

Downloaded from jb.asm.org at Wageningen UR Library on August 23, 2009

regression method by means of DynaFit 3.24 software (30), assuming Michaelis-Menten kinetics.

The optimum temperature and pH for oxidoreductase activity were determined by a standard assay at temperatures between 10 and 50°C; the buffer was replaced at 30°C with similar amounts of succinate HCl (pH 5.0 to 6.0), Bis-Tris-propane HCl (pH 6.25 to 9.0), and bis-Tris HCl (pH 5.75 to 7.25).

The sensitivity of the FAD oxidoreductase activity of StyA2B toward inhibitors (after 10 min of incubation) was tested by the standard assay with the following added (μM): styrene (2,000), thioanisole (2,000), styrene oxide (100 and 200), methylphenylsulfide (100 and 200), hydrogen peroxide (100), Mg^{2+} (20), Ca^{2+} (20), Fe^{2+} (100), Cd^{2+} (10), Hg^{2+} (10), Na_2EDTA (10,000), DTT (500), *o*-phenanthroline (10), metyrapone (100), mercaptoethanol (500), thiourea (10), or sodium azide (500). Metals were applied as chlorides or sulfates. In the case of Hg^{2+}, 0.4 mg of bovine serum albumin was added prior to the addition of NADH to avoid artificial complex formation. Reactivation after Cd^{2+} treatment was tested by incubation with 100 μM DTT for 10 min.

The oxygenase activity of recombinant StyA2B with styrene was measured by quantification of the reaction product. A typical oxygenase assay was performed in a 3-ml glass vial fitted with a Teflon-coated septum and placed in a continuously shaken (750 rpm) thermoblock. The standard reaction mixture contained the following in a final volume of 250 μl: 5 μmol Tris HCl (pH 7.5), 0.25 μmol DTT, 5% (vol/vol) glycerol, 37.5 μmol formate, 0.5 U formate dehydrogenase (from *Candida boidinii*; Fluka), 650 U catalase (from bovine liver; Fluka), 43.8 nmol NADH, 12.5 nmol FAD, 0.5 μmol styrene (100 mM in ethyl alcohol), and an appropriate amount of StyA2B (adapted from reference 44). After a 10-min preincubation at 30°C, the reaction was started by the addition of the substrate by means of a GC syringe (Hamilton). Samples (25 μl) were taken at different intervals, the reaction was quenched by the addition of the same volume of acetonitrile, and the samples were centrifuged (10,000 × *g*; 10 min) and subjected to reverse phase high-performance liquid chromatography (HPLC).

For the determination of oxygenase specificity, substitutions of similar concentrations of 4-chlorostyrene, 4-methylstyrene, dihydronaphthalene, and thioanisole were made for styrene. Reaction rates (measured in triplicate) were determined from the initial slope of product formation, and relative velocities were calculated by comparing the obtained specific activities to that for styrene (100%).

Formation of chiral epoxides by means of whole-cell biotransformation. Induced cells of *E. coli* BL21(pSRoA2B_P01) were harvested by centrifugation and resuspended in 20 ml 27 mM sodium-potassium phosphate (pH 7.3) to give a final OD_{600} of 20. After being transferred in a 250-ml baffled shaking flask, 2 mM glucose and 1 mM styrene or 4-chlorostyrene (100 mM in dimethylformamide) were added, and incubation took place at 37°C in a shaker (120 rpm) for 24 h. After the removal of cells by centrifugation, clear supernatants were subjected to solvent (3× 1 ml hexane) extraction. The combined organic phase sample was dried with anhydrous sodium sulfate and freed from the solvent under reduced pressure. When a final volume of approximately 50 μl was reached, the sample was subjected to chiral HPLC.

HPLC. Reverse phase HPLC analyses of products from StyA2B-mediated oxygenations were performed on a vertex column packed with Eurospher C_{18} (125-mm length by 4-mm internal diameter; 5-μm particle size; 100-Å pore size; Knauer, Germany). Acetonitrile-water was used as the mobile phase (1.0 ml min^{-1}). Styrene oxide (net retention volume, 1.78 ml; 60% [vol/vol] acetonitrile), 4-chlorostyrene oxide (2.74 ml; 60%), 4-methylstyrene oxide (2.45 ml; 60%), and methylphenylsulfoxide (0.89 ml; 50%) were separated in the isocratic mode, and dihydronaphthalene oxide (5.20 ml) was eluted during a linear gradient of 40 to 75% (vol/vol) acetonitrile over 11 ml. The retention volumes and UV spectra (200 to 400 nm) of all products were compared to those of authentic standards. Absorbance at 210 nm was used for quantification and was applied to multipoint calibrations.

For chiral HPLC and in order to separate (*R*)- and (*S*)-styrene oxides, a Nucleodex α-PM column (250-mm length by 4-mm internal diameter; Machery-Nagel, Germany) was used for the stationary phase in the isocratic mode (40% [vol/vol] methanol; 0.1% [vol/vol] triethyl ammonium acetate [pH 4.0]; 0.7 ml min^{-1}). Due to the lack of authentic standards, assignment of the (*S*)- and (*R*)-enantiomers of 4-chlorostyrene oxide (65.68 ml and 74.49 ml, respectively) was based on comparison to the retention behavior of the corresponding enantiomers of styrene oxide (51).

Nucleotide sequence accession number. The 8,965-bp genomic consensus sequence of p1CPS1 and p1CPS2 has been deposited at GenBank under accession no. FJ403049; also, see Fig. S1 in the supplemental material.

RESULTS AND DISCUSSION

Identification of two indole-oxidizing clones harboring putative monooxygenases of *R. opacus* 1CP. In an attempt to identify genes of chlorophenol hydroxylases by means of a clone library, partially Sau3AI-digested genomic DNA of *R. opacus* 1CP was cloned into the unique BamHI restriction site of pBluescript II KS(+). The obtained transformants were screened for their indigo formation ability on LB medium. The ability to oxidize indole (available from tryptophan by the action of an *E. coli* tryptophanase) to indigo is a property that is applicable for the detection of certain monooxygenase activities (26, 42). One single clone (p1CPS1) was found to react positively, growing as a dark-blue-centered colony. Preliminary sequence analysis of the 5,542-bp insert of that clone indicated the presence of two ORFs with high levels of similarity to a large number of monooxygenases. One of these monooxygenase-like genes was incomplete; thus, an overlapping clone, p1CPS2 (4,850-bp insert), was obtained by hybridization, using a DIG-labeled region of that ORF as a probe. Colonies of clone p1CPS2 showed phenotypic behavior similar to that of p1CPS1 in respect to the ability to generate indigo from indole.

***R. opacus* 1CP mineralizes styrene via styrene oxide and probably by an aerobic phenylacetic acid (PAA) pathway.** In order to confirm the first functional indications of the two monooxygenases encoded on the genomic fragment, strain 1CP was checked for its ability to mineralize styrene. Like benzene, toluene, and the xylenes, the hydrocarbon styrene behaves as a typical solvent, and due to an octanol-water partition coefficient below 4 ($\log P = 2.95$), it is extremely toxic for microorganisms (47). Accumulation within the cytoplasmic membrane followed by its disruption is the most likely mode of action. Lack of success at attempts to cultivate strain 1CP in liquid mineral medium in the presence of a styrene-saturated vapor phase can be attributed to this distinct sensitivity. However, after decreasing the size of the styrene aliquots that were frequently added through the evaporation adapter, this hydrocarbon was found to serve as the sole carbon and energy source for strain 1CP. Not surprisingly, the sizes of the added styrene aliquots could later be adapted for the growing culture. An OD_{600} of up to 1.5 was obtained for a supplied total styrene concentration of 10 mM.

An exponentially growing styrene culture was analyzed for intermediates by means of GC-MS in order to get information on the type of degradation pathway. Two metabolites, both with mass peaks of 120 *m/z* and a strong signal of 91 *m/z* for the tropylium ion $(C_7H_7)^+$ were detected in the aqueous culture supernatant. Both MS spectra and the retention behavior of these intermediates were shown to be identical to authentic references for styrene oxide and phenylacetaldehyde (data not shown; MS spectra are shown in Fig. S2 in the supplemental material). This observation strongly indicates that styrene is initially degraded by a monooxygenase-catalyzed epoxidation of the vinyl side chain. The resulting styrene oxide may then be further converted to phenylacetaldehyde by the action of an epoxystyrene isomerase (Fig. 2). Such a pathway of side chain oxygenation is the most common for the aerobic degradation of styrene and has been described for several strains of the proteobacterial genera *Pseudomonas* and *Xanthobacter* (reviewed by O'Leary and coworkers [43]). Taking into account

Downloaded from jb.asm.org at Wageningen UR Library on August 23, 2009

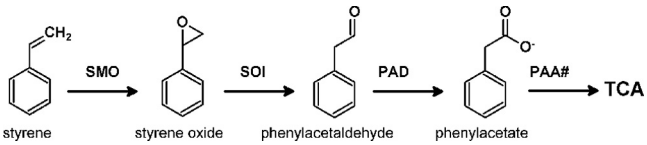

FIG. 2. Proposed styrene metabolic pathway via vinyl side chain oxygenation in *R. opacus* 1CP. The involved enzymes comprise SMO, styrene oxide isomerase (SOI), phenylacetaldehyde dehydrogenase (PAD), and multiple enzymes of phenylacetate degradation (PAA#) leading to intermediates of the tricarboxylic acid cycle (TCA).

this catabolic route, phenylacetaldehyde may be further oxidized to PAA by the action of a phenylacetaldehyde dehydrogenase. Attempts to detect PAA from the above culture supernatant of strain 1CP failed. However, PAA serves as a good growth substrate for *R. opacus* 1CP (5 mM PAA yielded an OD_{600} of 1.27), indicating the presence of a complete catabolic pathway for this compound.

Analysis of a 9-kb genomic fragment of strain 1CP harboring a hypothetical self-sufficient SMO. The overlapping inserts of p1CPS1 and p1CPS2 allowed the characterization of an entire 8,965-bp genomic region of strain 1CP harboring nine ORFs (Fig. 3a). Incomplete ORF1 encodes the N-terminal part of a protein with similarity to putative regulators of PAA metabolism (1, 17) (Table 2). Considering that styrene is usually degraded via side chain oxygenation to this intermediate (Fig. 2) (5), similarity to proteins involved in PAA degradation is not unexpected. Also relevant in this respect is ORF2, which encodes a putative 538-amino-acid (aa) AMP-dependent acyl coenzyme A (acyl-CoA) ligase. PAA-CoA ligases, which belong to this class of enzymes, are responsible for the degradation of PAA. ORF3, which may be transcribed with ORF2, encodes a 264-aa protein with a high level of similarity to a large number of putative short-chain dehydrogenases.

The two coding regions of the highest interest, ORF4 and ORF5, were obviously responsible for the indole-oxidizing activity of p1CPS1 and p1CPS2. ORF4 was designated *styA1*, since the deduced protein showed a high level of similarity to a large number of oxygenase subunits of putative two-component SMOs. The very few among them whose activity was experimentally proven are SMOs from pseudomonads (e.g., the main component, StyA, of *Pseudomonas fluorescens* strain ST [4]) or from an uncultured bacterium (subunit A [61]) (Table 2).

ORF5, which is cotranscribed and located directly downstream of ORF4, was found to be most remarkable, since the encoded protein seems to represent a fusion between an oxygenase and a flavin oxidoreductase. The N-terminal segment (105 to 108 identical amino acids over a length of 399 aa) of the deduced protein showed 26 to 27% sequence identity to oxygenase components of two-component SMOs from pseudomonads, whereas the C-terminal segment (51 to 54 identical amino acids over a length of 151 to 155 aa) was similar to the corresponding flavin reductase components of such systems (32 to 34% sequence identity). Accordingly, ORF5 was designated *styA2B*.

Incomplete ORFs 6 and 9 encode a 143-aa N-terminal and a 26-aa internal segment, respectively, of a hypothetical dienelactone hydrolase. Enzymes such as dienelactone hydrolase are usually involved in the modified *ortho*-cleavage pathway of chlorocatechols (41).

The encoded proteins of ORF7 and ORF8 are highly related to transposases (Table 2), and inverted repeats that possibly terminate the two slightly overlapping insertion elements were identified (for ORF7, 6575-TACTAGGGCGTGTCTCCCAATGATTTG-6601 and 7539-ATCATCCCGTACAGAGGGTTATCAAAC-7513; for ORF8, 7531-GCCCTACTACTGCAACGGCACTT-7553 and 8893-CGGCATCATGACGTTGCCGTGAA-8871). The transposons were obviously integrated one after another into the dienelactone hydrolase gene.

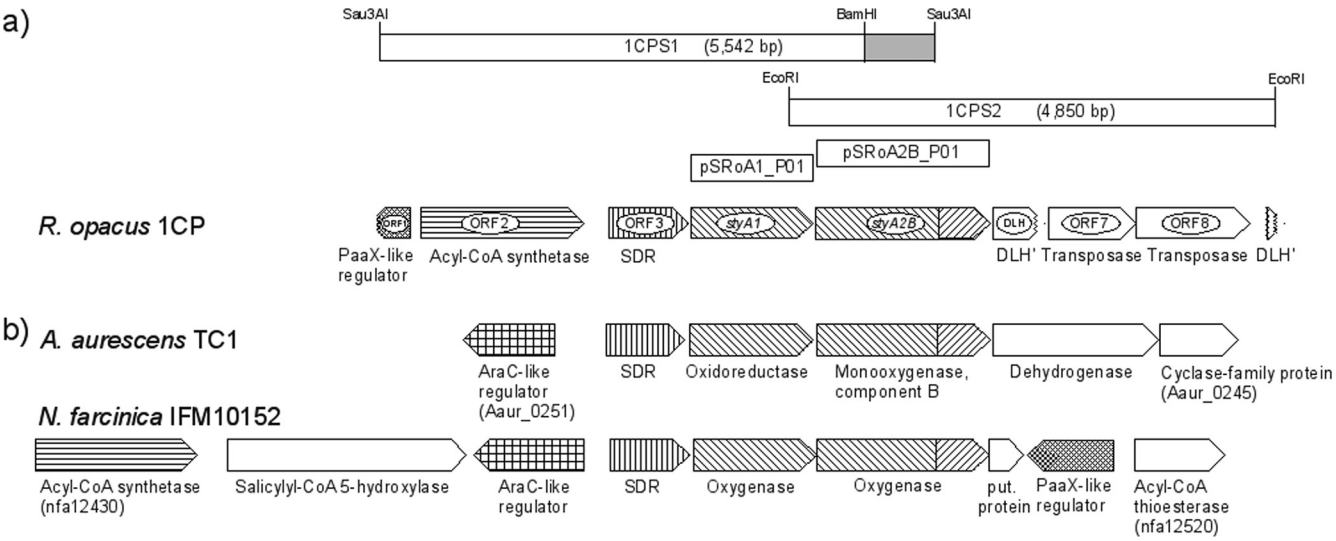

FIG. 3. Location of *styA1* and *styA2B* on the 8.965-kb region of genomic *R. opacus* 1CP DNA (a) and comparison to chromosomal regions of *A. aurescens* TC1 (CP000474) and *N. farcinica* IFM10152 (AP006618) (b), both harboring genes for similar putative self-sufficient monooxygenases. Inserts of p1CPS1, p1CPS2, and expression plasmids for *styA1* and *styA2B* are shown. Gray shading indicates a terminal 688-bp fragment of p1CPS1 used as a DIG-labeled probe for identification of p1CPS2. Locus tags are given for the first and last genes of the genomic regions compared. Identical hatching indicates a similar protein function. SDR, short-chain dehydrogenase; DLH′, dienelactone hydrolase; put., putative.

Downloaded from jb.asm.org at Wageningen UR Library on August 23, 2009

TABLE 2. Identified ORFs on the 8,965-bp consensus sequence of p1CPS1 and p1CPS2 inserts and similarities of deduced proteins

ORF (gene)	Product size (aa)[a]	Position of start-stop codon[a]	Gene product description (bacterium)[b]	NCBI accession designation	No. of identical amino acids/no. of amino acids in aligned region (% identity)
1	112[i]	337–1[i]	Hypothetical protein (*N. farcinica* IFM10152)	BAD56096	54/78 (69%)
			Repressor of PAA catabolism (*Saccharopolyspora erythraea* NRRL2338)	CAM02415	62/104 (59%)
			Putative transcriptional regulator; PaaX-like protein family (*A. aurescens* TC1)	ABM07064	34/79 (43%)
2	539	435–2051	AMP-dependent acyl-CoA synthetase (*S. erythraea* NRRL2338)	CAM02409	363/533 (68%)
			Putative acyl-CoA synthetase (*N. farcinica* IFM10152)	BAD56088	355/536 (66%)
			Putative acyl-CoA synthetase/AMP-fatty acid ligase (*A. aurescens* TC1)	ABM09333	326/535 (60%)
3	265	2312–3106	Short-chain dehydrogenase (*Burkholderia vietnamiensis* G4)	ABO59359	162/259 (62%)
			Short-chain dehydrogenase (*N. farcinica* IFM10152)	BAD56092	163/263 (61%)
			Short-chain dehydrogenase (*A. aurescens* TC1)	ABM07464	156/258 (60%)
4 (*styA1*)	407	3131–4351	Putative oxygenase (*N. farcinica* IFM10152)	BAD56093	296/406 (72%)
			Putative oxidoreductase (*A. aurescens* TC1)	ABM07034	275/408 (67%)
			Main component of SMO; StyA (*P. fluorescens* ST)	CAB06823	125/414 (30%)
			SMO large component (*Pseudomonas* sp. strain VLB120)	AAC23718	123/414 (29%)
5 (*styA2B*)	574	4387–6108	Putative oxygenase (*N. farcinica* IFM10152)	BAD56094	341/578 (58%)
			Putative monooxygenase component B (*A. aurescens* TC1)	ABM10099	311/583 (53%)
			SMO large component (*Pseudomonas* sp. strain VLB120)	AAC23718	107/399 (26%)
			SMO small component (*Pseudomonas* sp. strain VLB120)	AAC23719	51/155 (32%)
6 and 9[c]	143[i] and 26	6152–6580[i] and 8888–8965[i]	Putative dienelactone hydrolase (*Burkholderia cenocepacia* J2315)	CAR55985	98/166 (59%)
			Carboxymethylenebutenolidase (*Burkholderia xenovorans* LB400)	ABE35672	97/165 (58%)
			Carboxymethylenebutenolidase (*Burkholderia* sp. strain H160)	EDZ99576	97/167 (58%)
7	290	6707–7576	Putative transposase (*Rhodococcus* sp. strain RHA1)	ABG99655	263/275 (95%)
			Transposase (*R. opacus* R7)	ABH01025	171/199 (85%)
			Transposase; IS*4* family protein (*Mycobacterium vanbaalenii* PYR-1)	ABM11341	113/184 (61%)
8	378	7581–8714	Putative transposase (*Rhodococcus* sp. strain RHA1)	ABH00342	364/377 (96%)
			Transposase; IS4 family protein (*Frankia* sp. strain EAN1pec)	ABW12678	259/370 (70%)
			Putative transposase (*Streptomyces* sp. strain HK1)	ABY83494	204/359 (56%)

[a] A superscript "i" indicates an incomplete sequence.
[b] As given in the NCBI database.
[c] Continuation of ORF6; ORFs 6 and 9 were fused and analyzed for similarities as one amino acid sequence.

Localization of *styA2B*-like genes in other genomes. A BLAST search of StyA2B with the available sequence data allowed the identification of two other *styA2B*-like "merged" genes in the chromosomes of *Nocardia farcinica* IFM10152 and *Arthrobacter aurescens* TC1. The encoded proteins were designated as a putative oxygenase (BAD56094) and putative monooxygenase component B (ABM10099), respectively, and both were recently suggested to represent SMOs (60).

Comparison of adjacent ORFs to those found on the 9-kb genome fragment of strain 1CP yielded a number of structural homologies, giving at least a hint that StyA2B (*R. opacus* 1CP), BAD56094 (*N. farcinica* IFM10152), and ABM10099 (*A. aurescens* TC1) (Fig. 3b) may fulfill a similar physiological function, which is probably part of styrene metabolism. Most remarkably, the genes of the hypothetical fusion SMOs of strains IFM10152 and TC1 are both located directly adjacent to an ORF encoding a protein highly similar to the N-terminal oxygenase-like segment of BAD56094 and ABM10099, respec-

Downloaded from jb.asm.org at Wageningen UR Library on August 23, 2009

tively, a finding that is consistent with the *styA1-styA2B* system of *R. opacus* 1CP, and as in strain 1CP, the ORFs of strains IFM10152 and TC1 are both potential subjects of cotranscription. Another striking similarity in all three organisms is the presence of an adjacent ORF encoding a short-chain dehydrogenase-like protein of hitherto unknown function. The presence of additional ORFs encoding a putative PaaX-like regulator and a putative acyl-CoA synthetase is another striking similarity between strains 1CP and IFM10152, which led to the assumption that StyA1/StyA2B may in fact be responsible for the initial degradation of styrene, which in the most common degradation pathway yields PAA as an intermediate (Fig. 2). It should be mentioned that although a PaaX-like regulator and an acyl-CoA synthetase of *A. aurescens* TC1 are located elsewhere on the chromosome (Aaur_4024 and Aaur_4030), the two genes are located close to each other.

Structural properties of StyA1 and StyA2B and their relatedness to other SMOs. From the above results, it seems likely that *styA1* and *styA2B* encode components of SMOs. A multiple-sequence alignment of StyA1 and StyA2B with SMOs of known function revealed the presence of conserved sequence motifs typical for a mechanistic involvement of flavins and nicotinamide adenine dinucleotides (Fig. 4). The FAD-binding fingerprints GxGxxG, GG, and Dx6G (15) were found in both StyA1 and StyA2B proteins at amino acid positions 8, 118 (StyA1, 117), and 139 (StyA1, 138), respectively. In addition, Ser46 and Pro299 of StyA2B as well as Pro298 of StyA1 likely correspond to highly conserved amino acids necessary for the activity of SMOs (15). Pro299 (StyA2B) and Pro298 (StyA1) both belong to a Gdx6P sequence motif important for FAD/NAD(P) interaction. Finally, the residual C-terminal part of StyA2B (approximate position, aa 414 to 573; 160 aa) is highly conserved and similar to those of flavin reductases, which use NAD(P)H as a cofactor in order to reduce flavin-containing cosubstrates. Note that no flavin-binding motif could be found in the reductase domain.

Comparison of the fusion with the C-terminal StyA and N-terminal StyB regions indicates that fused SMOs lack 10 (*Pseudomonas* spp.) to 14 (*Delftia acidovorans*) amino acids of the N-terminal part of StyB.

The phylogenetic relatedness of StyA2B was determined with respect to its oxygenase and oxidoreductase moiety (Fig. 5). Since so far only a very few two-component SMOs have been assigned by experimental evidence, most sequences taken from genomes represent monooxygenases of unknown specificity. The dendrogram in Fig. 5 indicates the highest level of relatedness among all three hypothetical one-component SMOs from *R. opacus* 1CP (StyA2B), *N. farcinica* IFM10152 (BAD56094), and *A. aurescens* TC1 (ABM10099) for both oxygenase and flavin oxidoreductase moieties. Together with StyA1 from *R. opacus* 1CP, the single oxygenase components of these organisms form a separate cluster that is distinct from, but still closely related to, the cluster of the N-terminal oxygenase moieties of one-component SMOs. This finding suggests that the presumed fusion of oxygenase and flavin oxidoreductase moieties occurred only in the SMO branch of these *Actinobacteria* and is not an ancient feature among SMOs (Fig. 5).

Overexpression, purification. and size determination of recombinant His_{10}-StyA1 and His_{10}-StyA2B in *E. coli*. In order to characterize StyA1 and StyA2B in more detail, both genes were amplified with specific primers and cloned into a pET16b (Novagen) vector derivative to give pSRoA1_P01 and pSRoA2B_P01, respectively. Expression of the His_{10}-tagged proteins was performed in *E. coli* BL21, and the efficiency of expression was tested at 20°C, 30°C, and 37°C in the presence of 0.1 mM and 1.0 mM of IPTG. During the induction period, a green-to-blue coloration of the cultures, faint for pSRoA1_P01 and distinct for pSRoA2B_P01, was the first evidence of the expression of active monooxygenases. In fact, SDS-PAGE of the cytosolic and insoluble fraction indicated successful expression of soluble His_{10}-StyA2B, of which the highest yields were obtained by induction at 20°C in the presence of 0.1 mM IPTG. The recombinant protein appeared as a dominant band at around 65 kDa, which fits well with the calculated size of 64,329 Da (Fig. 6a).

His_{10}-StyA2B was purified to homogeneity by Ni chelate chromatography. As a result, 32 mg of His_{10}-StyA2B, accounting for 11% of the total protein, was obtained from *E. coli* BL21(pSRoA2B_P01). Storage of the protein at −20°C in the presence of glycerol-DTT proved to be the most gentle method to minimize inactivation.

Size exclusion chromatography of the final His_{10}-StyA2B preparation yielded a single symmetrical protein peak corresponding to a molecular mass of 138 ± 2 kDa for the native enzyme, which indicates a homodimeric structure. Interestingly, a similar organization was reported for both the oxygenase component StyA and the oxidoreductase component StyB of the two-component SMO from *Pseudomonas* sp. strain VLB120 (44).

In the case of His_{10}-StyA1, SDS-PAGE produced a dominant band at 44.8 ± 0.5 kDa (calculated size, 46,537 Da), indicating recombinant expression. Unfortunately, the protein could be found only in the insoluble cell fraction, indicating the exclusive formation of inclusion bodies. Neither reducing the growth temperature down to 20°C nor decreasing the IPTG concentration to 0.1 mM brought about a detectable yield of active enzyme in the cytosol (data not shown).

StyA2B shows NADH-specific FAD oxidoreductase activity. Due to its protein sequence similarities, recombinant StyA2B was characterized as both a flavin reductase and an oxygenase. The oxidoreductase-like moiety of StyA2B was analyzed for its specificity toward several flavin-containing electron acceptors and the electron donor NAD(P)H (Table 3). As in the two-component SMO from *Pseudomonas* sp. strain VLB120 (44), activity was specifically restricted to NADH, whereas FAD, FMN, and riboflavin were shown to serve as flavin substrates. The utilization of different flavins as electron acceptors is typical for NADH-dependent flavin oxidoreductases that do not contain a tightly bound flavin (44), and spectrophotometrical analysis confirmed that StyA2B shares this characteristic (see below). On the other hand, flavin reductases that harbor a flavin prosthetic group use a second free flavin for electron transfer (28). FAD, FMN, and riboflavin were reduced by His_{10}-StyA2B with comparable turnover numbers (3.0 to 5.2 s^{-1}), whereas the Michaelis constants for these compounds decreased in the following order: that for FMN (67 μM) was greater than that for FAD (26 μM), which was greater than that for riboflavin (23 μM). Affinity constants in the micromolar range indicate that these flavins act as weakly bound cofac-

Downloaded from jb.asm.org at Wageningen UR Library on August 23, 2009

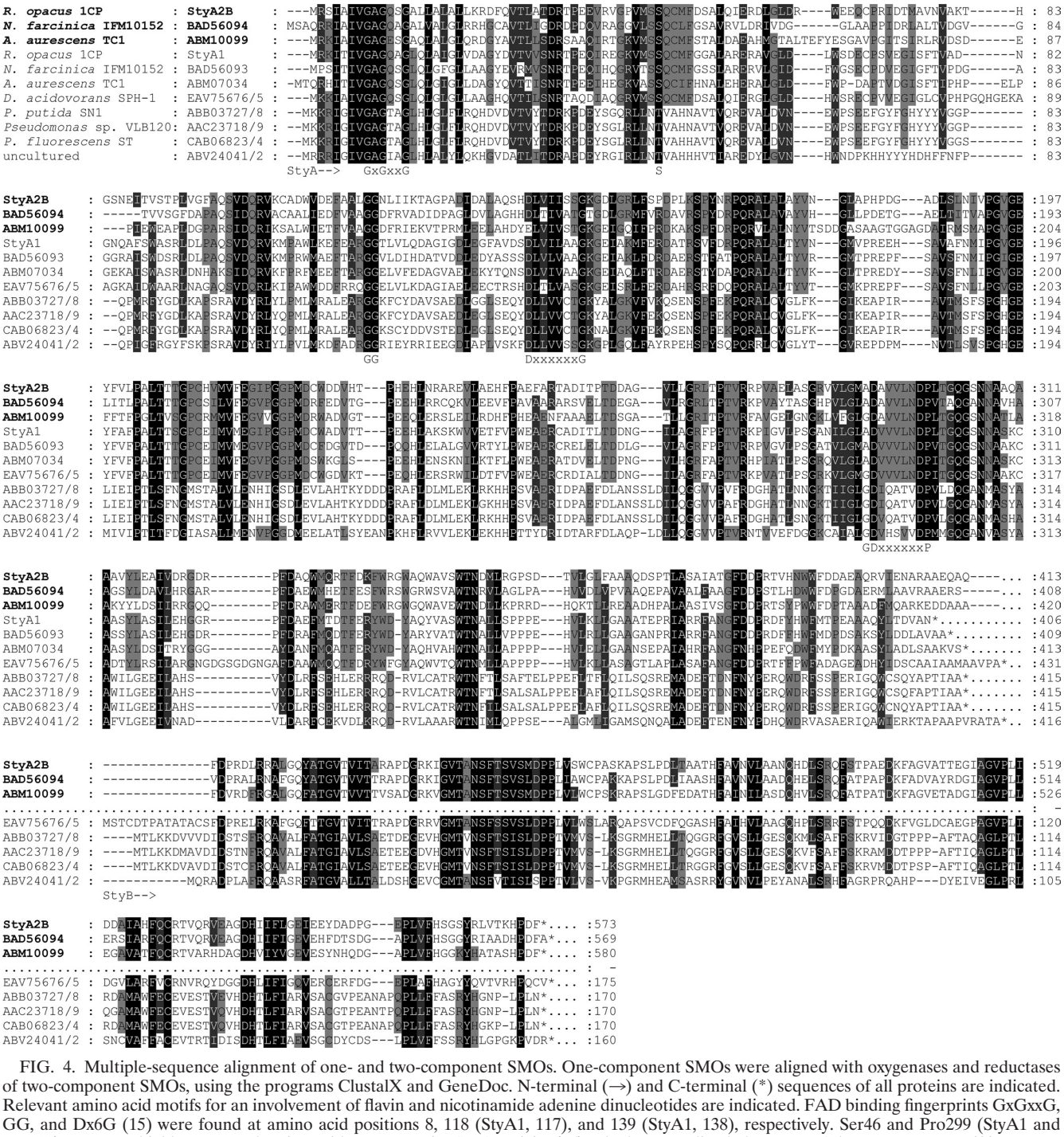

FIG. 4. Multiple-sequence alignment of one- and two-component SMOs. One-component SMOs were aligned with oxygenases and reductases of two-component SMOs, using the programs ClustalX and GeneDoc. N-terminal (→) and C-terminal (*) sequences of all proteins are indicated. Relevant amino acid motifs for an involvement of flavin and nicotinamide adenine dinucleotides are indicated. FAD binding fingerprints GxGxxG, GG, and Dx6G (15) were found at amino acid positions 8, 118 (StyA1, 117), and 139 (StyA1, 138), respectively. Ser46 and Pro299 (StyA1 and Pro298) represent highly conserved amino acids necessary for SMO activity (15). The latter proline belongs to a Gdx6P sequence motif important for FAD/NAD(P) interaction. The C-terminal reductase fragment (aa 414 to 573) of StyA2B is similar to flavin reductases which utilize NAD(P)H as a coenzyme to reduce FMN/FAD (not shown). Shading indicates different degrees of conserved amino acid similarity (black, 100%; dark gray, 80%; gray, 60%).

tors. Under the given reaction conditions, FAD proved to be the most favored electron acceptor for StyA2B, with a catalytic efficiency of 0.2 s^{-1} μM^{-1}. This value is about twenty times lower than the corresponding value reported for StyB from *Pseudomonas* sp. strain VLB120 (44), a fact which can be attributed to the considerably lower turnover rate of StyA2B.

Relevance of bound flavin, heme, and metals for the oxidoreductase. As mentioned above, flavin is used as an exchangeable substrate and not as a prosthetic group, which raises further questions about StyAB oxidoreductase activity. No dependence was observed between the FAD oxidoreductase activity of StyA2B and the presence of styrene, which indicates that in the absence of an aro-

Downloaded from jb.asm.org at Wageningen UR Library on August 23, 2009

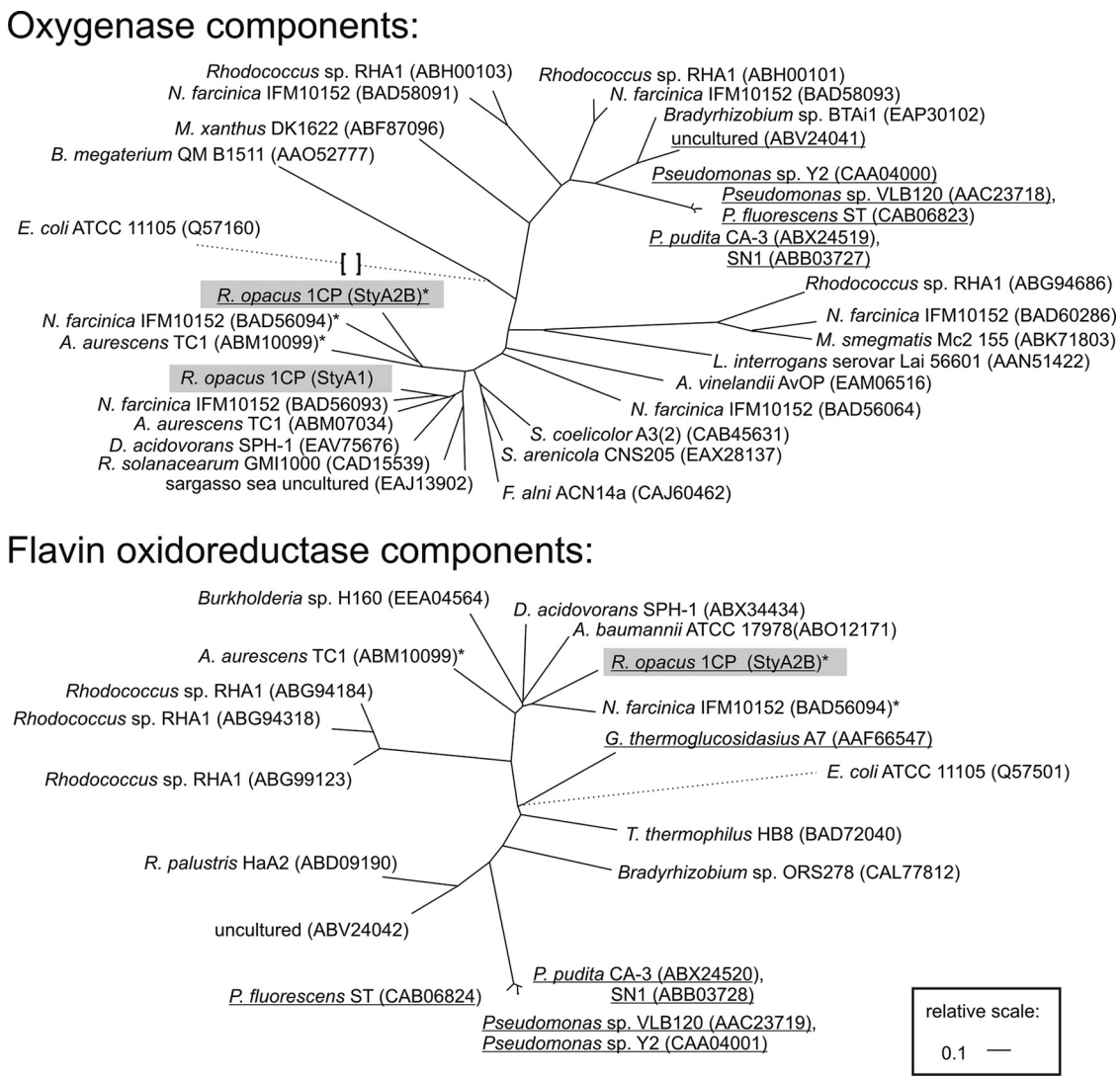

FIG. 5. Dendrograms showing the relationship of StyA2B to other (putative) single- and two-component (styrene) monooxygenases. Distance trees were created with respect to the oxygenase- and flavin oxidoreductase-like moieties of StyA2B with the software programs ClustalX (version 1.8) (19, 55) and GeneDoc (version 2.6.003) and the PHYLIP 3.66 package (PROTDIST and FITCH) (16). The oxygenase and reductase components of 4-hydroxyphenylacetate 3-monooxygenase served as the outgroup. Enzymes from *R. opacus* 1CP are shaded gray, those with reported activity are underlined, and putative self-sufficient one-component SMOs are marked with asterisks. *M. xanthus*, *Myxococcus xanthus*; *D. acidovorans*, *Delftia acidovorans*; *R. solanacearum*, *Ralstonia solanacearum*; *R. palustris*, *Rhodopseudomonas palustris*; *P. fluorescens*, *Pseudomonas fluorescens*; *P. putida*, *Pseudomonas putida*; *M. smegmatis*, *Mycobacterium smegmatis*; *L. interrogans*, *Leptospira interrogans*; *A. vinelandii*, *Azotobacter vinelandii*; *S. coelicolor*, *Streptomyces coelicolor*; *S. arenicola*, *Salinispora arenicola*; *F. alni*, *Frankia alni*; *A. baumannii*, *Acinetobacter baumannii*; *T. thermophilus*, *Thermus thermophilus.*

matic substrate, StyA2B acts as an NADH oxidase. In fact, hydrogen peroxide could be detected from such conversions (data not shown). This uncoupling reaction is typical for two-component SMOs (25, 44). On the other hand, the complete absence of NADH oxidase activity in StyA2B without the presence of FAD clearly indicates the necessity of an external flavin electron acceptor.

In addition to the need for an external electron acceptor, StyA2B was analyzed for the presence of tightly bound flavin. For that purpose, the absorbance at 450 nm of homogeneous His_{10}-StyA2B was compared to that of an equimolar concentration of free FAD (Fig. 6b). An absorption ratio between 1:14 and 1:20 did not indicate the presence of bound flavin, at least in a stoichiometric amount. This property distinguishes StyA2B from flavin reductase PheA2 (28, 58), which harbors a tightly bound FAD.

The absence of heme groups was confirmed by the insensitivity of StyA2B toward metyrapone, an effective inhibitor of cytochrome P450 enzymes (53). This result correlates with the optical properties reported above and with the StyA2B protein sequence in which no heme binding motif could be found.

His_{10}-StyA2B was subjected to inhibition studies in order to reveal information about catalytically relevant groups or species. Chelating agents such as EDTA and *o*-phenanthroline had no noticeable effect on FAD-reducing activity, indicating that divalent anions are not necessary for catalysis. Accordingly, neither 20 μM of Ca^{2+} or Mg^{2+} nor 100 μM Fe^{2+}

Downloaded from jb.asm.org at Wageningen UR Library on August 23, 2009

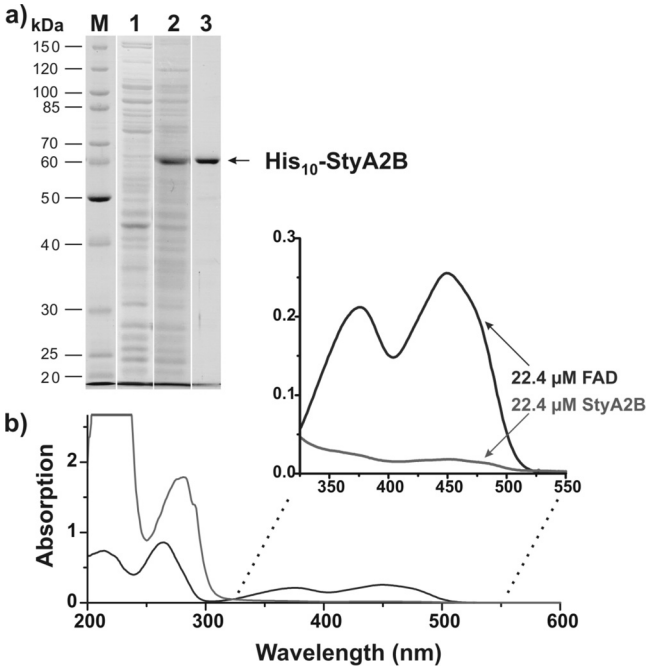

FIG. 6. SDS-PAGE (a) and UV-visible absorption spectrum (b) of His_{10}-StyA2B. (a) A 10% polyacrylamide gel was loaded as follows: lane M, PageRuler 10- to 200-kDa protein ladder (Fermentas); lane 1, crude extract of noninduced *E. coli* BL21(pSRoA2B_P01); lane 2, crude extract of induced *E. coli* BL21(pSRoA2B_P01); lane 3, 1.6 μg His_{10}-StyA2B from Ni chelate chromatography. (b) UV-visible absorption spectra of 22.4 μM purified His_{10}-StyA2B and a similar concentration of FAD in 10 mM Tris HCl (pH 7.5).

affected activity significantly. The insignificance of metals was confirmed by atom emission spectroscopy, during which no noticeable amount of Fe, Cu, Mn, Zn, Ni, or any other di- or trivalent metal was determined.

Not surprisingly, incubation of StyA2B with 10 μM Hg^{2+} or Cd^{2+} resulted in considerable decreases, 64% and 44%, respectively, in oxidoreductase activity. This effect is likely to be attributed to oxidation-sensitive cysteine residues, since significant inactivation (26%) was also observed for hydrogen peroxide. Accordingly, reducing agents like mercaptoethanol and DTT did not lower oxidoreductase activity, and a surplus of the latter compound was shown to fully abolish the inhibiting effect of Cd^{2+} ions. Interference relevant for further kinetic studies was shown for substrates and products of the oxygenase moiety of StyA2B. In the presence of 2 mM styrene or thioanisole (later shown to be favored oxygenase substrates for StyA2B), as well as 200 μM styrene oxide or methylphenylsulfoxide, only 50 to 80% of the FAD oxidoreductase turnover rate was observed.

Similar results in respect to the relevance of metals, the impact of certain inhibitors, and the absence of tightly bound flavin were reported for the two-component SMO from *Pseudomonas* sp. strain VLB120 (44). Thus, StyA2B indeed seems to represent a simple fusion between the moieties of a classical two-component SMO without a noticeable change in catalytically relevant groups.

Parameters affecting His_{10}-StyA2B activity. Initial attempts to remove the histidine tag from the recombinant His_{10}-StyA2B by proteolytic treatment with factor Xa (3.3 U $nmol^{-1}$ His-StyA2B; 21°C; 18 h) resulted in a drastic decrease of about 80% in FAD oxidoreductase activity. As a consequence, biochemical characterizations were performed with the His-tagged protein, keeping in mind that the N-terminal modification might influence catalytic behavior.

The optimum temperature for FAD oxidoreductase activity of recombinant StyA2B is about 37°C (Fig. 7b). The pH dependence of FAD oxidoreductase activity was determined, and the maximum pH was found to be 6.25 in Bis-Tris HCl (Fig. 7a). For a certain pH, it was observed that activity was greatly dependent on the applied buffer system.

Overall, the chosen standard assay conditions (30°C; Tris HCl; pH 7.5) were suboptimal and led to a limitation of activities to about 25% of the theoretical performance; however, these parameters reflect efforts to minimize acid-catalyzed epoxide hydrolysis and substrate evaporation.

StyA2B acts as an oxygenase with specificity for styrene and structurally related compounds. The monooxygenase activity and specificity of StyA2B were investigated with a coupled-enzyme assay in which the flavin oxidoreductase activity of StyA2B was used to generate reduced FAD. In addition, formate dehydrogenase-formate and catalase were included for the regeneration of NADH and for the removal of hydrogen peroxide, respectively. Care was taken that neither the NADH regeneration system nor the substrate and oxygen concentration was limiting to the monooxygenase activity.

Styrene, 4-chlorostyrene, and 4-methylstyrene all proved to be suitable substrates for recombinant His_{10}-StyA2B and were converted to the corresponding styrene oxides with specific activities of 6 to 19 mU mg^{-1} (Table 4). Epoxidation of the parent compound by whole-cell biotransformation with *E. coli* BL21(pSRoA2B_P01) was shown to be highly enantioselective, yielding (*S*)-styrene oxide in >94% enantiomeric excess (e.e.). Perceptibly lower enantioselectivity was shown for

TABLE 3. Kinetic parameters for FAD oxidoreductase activity of StyA2B toward different flavins (electron acceptors) and electron donors[a]

Electron donor (concn [μM])	Electron acceptor (concn [μM])	K_m (μM)	V_{max} (U mg^{-1})	k_{cat} (s^{-1})	$k_{cat}\,K_m^{-1}$ (s^{-1} μM^{-1})	% Relative $k_{cat}\,K_m^{-1}$
NADH (17.5–175)	FAD (50)	58 ± 9	3.7	3.9 ± 0.3	0.068	100
NADPH (175)	FAD (50)	ND	<0.01	ND	ND	ND
NADH (175)	FAD (4–60)	26 ± 2	4.9	5.2 ± 0.2	0.203	100
NADH (175)	Riboflavin (4–60)	23 ± 2	2.8	3.0 ± 0.1	0.131	64
NADH (175)	FMN (4–60)	67 ± 22	4.5	4.8 ± 1.0	0.071	35

[a] Activities were determined by the standard flavin oxidoreductase assay, applying 16.1 μg of His_{10}-StyA2B from *R. opacus* 1CP. K_m and V_{max} were calculated by the initial rate method and nonlinear regression analysis (DynaFit, version 3.28.059; curves are presented in Fig. S3 in the supplemental material) (30). ND, not determined.

Downloaded from jb.asm.org at Wageningen UR Library on August 23, 2009

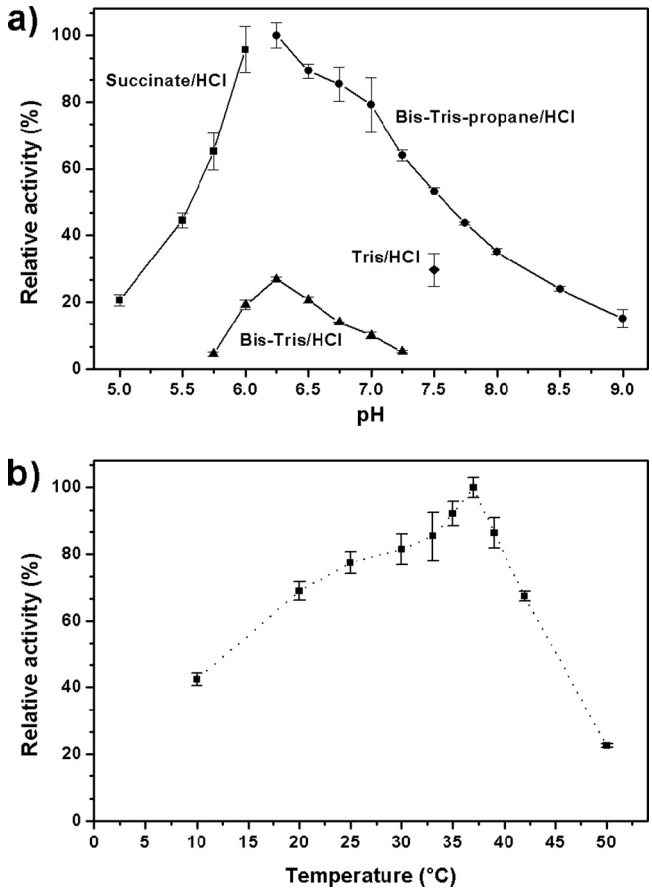

FIG. 7. pH (a) and temperature (b) dependence of the FAD oxidoreductase activity of StyA2B. The standard assay for flavin oxidoreductase activity was performed, applying the recombinant His_{10}-tagged protein in 20 mM of the appropriate buffer at 30°C (a) or in 20 mM Tris HCl (pH 7.5) (b) at various temperatures. Each datum point indicates the relative activity derived from triplicate measurements.

4-chlorostyrene, which yielded the (*S*)-epoxide in 82% e.e. Two-component SMOs from pseudomonads were reported to possess enantioselectivities of >98% e.e. toward these substrates (21, 60); however, the relative activities of styrene(s) are comparable to those for StyA2B. This is also true for the conversion of dihydronaphthalene (one of the best substrates of StyA/StyB [21]) and thioanisole (Table 4). Sulfoxidation of the latter to phenylmethylsulfoxide seems to be a common property among SMOs. No activity was measured for ethylbenzene, and the inability of StyA2B to convert acetophenone excluded a hydroxylase or a Baeyer-Villiger oxygenase.

In contrast to the similarities in substrate specificity, the specific monooxygenase activities of recombinant StyA2B from *R. opacus* 1CP were found in general to be at least one order of magnitude lower than those ones reported for StyA/StyB (21, 44) and SMO/PheA (60) (Table 4).

Conclusions. The evolution of enzymes develops from single active units toward complex multifunctional systems (48). Gene fusion is probably the simplest of the processes that enhance the overall complexity of a discrete protein by combining different functionalities of its ancestors. Compensation for the so-called phenomenon of intracellular crowding (10), benefiting kinetically by the close proximity of active sites (38), and coordinated regulation of expression that prevents metabolic cross talk between competing pathways are the major driving forces of multifunctional enzyme systems.

The self-sufficient SMO StyA2B from *R. opacus* 1CP described herein is likely to be an example of such an evolutionary process in which both genes of two-component SMOs encoding an oxygenase (StyA2) and a flavin oxidoreductase subunit (StyB) have been merged. StyA2B is able to oxidize styrene and structurally related compounds to the corresponding oxides at the expense of NADH. An externally provided flavin-containing cofactor that must first be reduced by the reductase domain is necessary as an electron mediator in order to activate dioxygen. The specificities of StyA2B toward the oxygenation substrates styrene, dihydronaphthalene, and phenylmethylsulfide strongly resemble those of oxygenases of reported two-component SMOs (44, 60). The same is true for the oxidoreductase specificity of StyA2B for electron donors [NAD(P)H] and electron acceptors (FAD, FMN, and riboflavin) compared to those of reductases of two-component SMOs (44). In addition, the absence of heme groups and metal ions and the weak binding of flavin in the recombinant His-tagged fusion protein correlate with the StyA/StyB system of *Pseudomonas* sp. strain VLB120 (44) and indicate that catalytically relevant groups are basically similar. The relatively low affinity of the oxidoreductase domain of StyA2B toward several flavin-containing cofactors indicates a weak binding of these cofactors, which is consistent with the absence of flavin binding sequence motifs and is probably a result of the isoalloxazine ring, not the nucleotide groups, as with most other flavoproteins, being favored for recognition. Another alternative binding mechanism of the oxidoreductase is likely to exist for NADH. This cofactor might bind in a solvent-accessible groove, adopting an unusual folded conformation with ring stacking, as was recently shown for a flavin reductase PheA2 of *Geobacillus thermoglucosidasius* A7 (58).

The low specific activity of StyA2B was an unexpected finding for this first type of fusion between a flavin-dependent monooxygenase and a flavin reductase. FAD-reducing and styrene-oxidizing activities of StyA2B were determined to be one to two orders lower than the corresponding values for the StyA/StyB system of strain VLB120. This is especially unexpected considering the situation in P450 monooxygenases, for which such fusions are more often found. The first and by far best-characterized representative of these cytochrome P450 fusions is the $P450_{BM3}$ fatty acid hydroxylase of *Bacillus megaterium*, in which the P450 domain is merged to an eukaryotic-like cytochrome P450 reductase (40). Like most other recently identified P450-redox partner fusion enzymes, these systems are characterized by enhanced catalytic efficiency (7, 8, 39). Whereas the K_m values of $P450_{BM3}$ for several fatty acid substrates are comparable to those of eukaryotic fatty acid hydroxylases, the turnover rates for hydroxylation (up to 270 s^{-1}) are at least two orders higher than those observed for the latter group of enzymes. In the fused BM3 system, the proximity of the FMN and heme domain ensures an increase in the productivity of the interaction, thus reducing the rate of unproductive decomposition of the unstable ferrous-oxygen–P450 complex and the formation of oxidative stress (38, 39).

The lack of structural data for StyA2B does not allow a

Downloaded from jb.asm.org at Wageningen UR Library on August 23, 2009

TABLE 4. Substrate specificity and stereoselectivity of StyA2B oxygenase activity and comparison to data of oxygenases from two-component SMOs

Substrate	Product	StyA2B (*R. opacus* 1CP)[a,e]			StyA and StyB (*Pseudomonas* sp. strain VLB120)[b,e]			SMO (unknown metagenome) and PheA2 (*G. thermoglucosidasius*)[c,e]		
		Oxygenase activity (U mg^{-1})	Favored enantiomer	e.e. (%)	Oxygenase activity (U mg^{-1})	Favored enantiomer	e.e. (%)	Oxygenase activity (U mg^{-1})	Favored enantiomer	e.e. (%)
Styrene 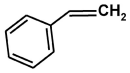	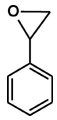	0.019	(*S*)	>94	0.268 0.204 2.1[d]	(*S*) (*S*) (*S*)	98.0	0.80	(*S*)	>99
4-Chlorostyrene 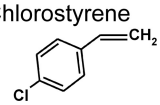	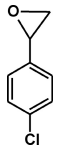	0.011	ND	>82	0.312	ND	98.1	0.23	(*S*)	>99
4-Methylstyrene 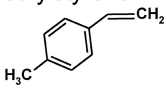	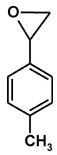	0.006	ND		0.312	ND	ND	ND	ND	ND
Dihydronaphthalene 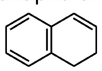	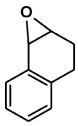	0.011	ND		0.376	ND	98.9	ND	ND	ND
Methylphenylsulfide (thioanisole) 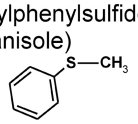	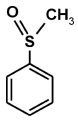	0.012	ND		0.226	ND	26	0.11	(*R*)	75

[a] Oxygenase and FAD oxidoreductase components (hosts). Data were obtained from this study.
[b] StyA (*Pseudomonas* sp. strain VLB120) is the oxygenase component (host); StyB (*Pseudomonas* sp. strain VLB120) is the FAD oxidoreductase component (host). StyB activity was replaced by electrochemical FAD regeneration. From references 21 and 44.
[c] SMO (unknown metagenome) is the oxygenase component (host); PheAZ (*G. thermoglucosidasius*) is the FAD oxidoreductase component (host). From reference 60.
[d] Data were obtained from recombinant enzymes and an optimized StyA/StyB ratio (44).
[e] ND, not determined.

prediction of the distance between the styrene binding pocket and the flavin-reducing site. Nevertheless, because of the instability of reduced flavin and the rate-limiting diffusion of this cofactor between the active sites of reductase and oxygenase, fusion proteins should be kinetically favored in a similar way, as was observed for $P450_{BM3}$. There may be several reasons for the observed contrary effect, of which the most likely ones could be partial misfolding of the recombinant protein, weak flavin binding, or structural interference of the N-terminal His tag. With respect to the unexpectedly low oxygenating activity, a hitherto overlooked role of the neighboring gene *styA1* comes into focus. The encoded protein, a putative styrene oxygenase component of a two-component SMO system, needs a specific FAD oxidoreductase counterpart for activity. Genes of two-component SMOs are typically closely located (1, 5), which is not true of *R. opacus* 1CP and *A. aurescens* TC1. Moreover, no *styB*-like gene could be identified on the basis of sequence similarity in strain TC1. Since StyA2B represents a merged StyB variant, a productive interaction with StyA1 is likely and may yield additional oxygenating activity. In addition to structural investigations of the StyA2B enzyme, a closer look at the synergetic effects between these proteins will be necessary in order to understand the evolutionary benefit of this novel fusion protein.

StyA2B is the first active representative of a self-sufficient SMO; however, similar fusion proteins were found in *A. aurescens* TC1 and *N. farcinica* IFM10152 (60). Like *R. opacus* 1CP, both species belong to the high-GC gram-positive phylum *Actinobacteria*. Comparison of the localization of *styA2B* with the corresponding genomic regions of the above organisms gave further evidence that a similar physiological function in styrene metabolism via PAA can be expected. The observation that virtually no fusion proteins of noticeable similarity are encoded within the sequenced genomes of gram-negative bacteria might indicate that self-sufficient SMOs may have evolved in and are a special feature of gram-positive prokaryotes. This assumption is not an unlikely hypothesis, since evidence of independent evolution of metabolic pathways between proteobacteria and *Actinobacteria* are frequently found, e.g., in the pathways of chlorocatechols (12, 37), catechol (11, 13), and protocatechuate (14).

SMOs represent only a small proportion of flavoprotein monooxygenases (57, 60), and among SMOs that are distributed with a genome frequency of 0.068 (21 SMOs from 309

Downloaded from jb.asm.org at Wageningen UR Library on August 23, 2009

genomes [57]), one-component SMOs form a novel class of flavin-dependent monooxygenases. Regardless of the low specific activity of the herein reported recombinant His_{10}-StyA2B, this subclass of SMOs should be further characterized. The activities of wild-type and mutant enzymes, the efficiency of flavin transfer, the interaction of StyA2B and StyA1, and biotechnological applicability are especially valuable targets of future study.

ACKNOWLEDGMENTS

This work was kindly supported by a predoctoral fellowship from the Deutsche Bundesstiftung Umwelt.

We thank Silke Tesch and Philipp Rathsack (Department of Analytical Chemistry, TU Bergakademie Freiberg) for ICP-AES- and GC-MS analysis, respectively.

REFERENCES

1. **Alonso, S., D. Bartolomé-Martin, M. del Álamo, E. Díaz, J. L. García, and J. Perera.** 2003. Genetic characterization of the styrene lower catabolic pathway of *Pseudomonas* sp. strain Y2. Gene **319:**71–83.
2. **Altschul, S. F., T. L. Madden, A. A. Schäffer, J. Zhang, Z. Zhang, W. Miller, and D. J. Lipman.** 1997. Gapped BLAST and PSI-BLAST: a new generation of protein database search programs. Nucleic Acids Res. **25:**3389–3402.
3. **Altschul, S. F., W. Gish, W. Miller, E. W. Myers, and D. J. Lipman.** 1990. Basic local alignment search tool. J. Mol. Biol. **215:**403–410.
4. **Beltrametti, F., A. M. Marconi, G. Bestetti, E. Galli, M. Ruzzi, and E. Zennaro.** 1997. Sequencing and functional analysis of styrene catabolism genes from *Pseudomonas fluorescens* ST. Appl. Environ. Microbiol. **63:**2232–2239.
5. **Bestetti, G., P. Di Gennaro, A. Colmegna, I. Ronco, E. Galli, and G. Sello.** 2004. Characterization of styrene catabolic pathway in *Pseudomonas fluorescens* ST. Int. Biodeterior. Biodegradation **54:**183–187.
6. **Bradford, M. M.** 1976. A rapid and sensitive method for the quantitation of microgram quantities of protein utilizing the principle of protein-dye binding. Anal. Biochem. **72:**248–254.
7. **Brodhun, F., C. Göbel, E. Hornung, and I. Feussner.** 2009. Identification of PpoA from *Aspergillus nidulans* as a fusion protein of a fatty acid heme dioxygenase/peroxidase and a cytochrome P450. J. Biol. Chem. **284:**11792–11805.
8. **De Mot, R., and A. H. A. Parret.** 2002. A novel class of self-sufficient cytochrome P450 monooxygenases in prokaryotes. Trends Microbiol. **10:**502–508.
9. **Dorn, E., M. Hellwig, W. Reineke, and H.-J. Knackmuss.** 1974. Isolation and characterization of a 3-chlorobenzoate degrading pseudomonad. Arch. Microbiol. **99:**61–70.
10. **Ellis, R. J.** 2001. Macromolecular crowding: obvious but underappreciated. Trends Biochem. Sci. **26:**597–604.
11. **Eulberg, D., and M. Schlömann.** 1998. The putative regulator of catechol catabolism in *Rhodococcus opacus* 1CP—an IclR-type, not a LysR-type transcriptional regulator. Antonie van Leeuwenhoek **74:**71–82.
12. **Eulberg, D., E. M. Kourbatova, L. A. Golovleva, and M. Schlömann.** 1998. Evolutionary relationship between chlorocatechol catabolic enzymes from *Rhodococcus opacus* 1CP and their counterparts in proteobacteria: sequence divergence and functional convergence. J. Bacteriol. **180:**1082–1094.
13. **Eulberg, D., L. A. Golovleva, and M. Schlömann.** 1997. Characterization of catechol catabolic genes from *Rhodococcus erythropolis* 1CP. J. Bacteriol. **179:**370–381.
14. **Eulberg, D., S. Lakner, L. A. Golovleva, and M. Schlömann.** 1998. Characterization of a protocatechuate catabolic gene cluster from *Rhodococcus opacus* 1CP: evidence for a merged enzyme with 4-carboxymuconolactone-decarboxylating and 3-oxoadipate enol-lactone-hydrolyzing activity. J. Bacteriol. **180:**1072–1081.
15. **Feenstra, K. A., K. Hofstetter, R. Bosch, A. Schmid, J. N. M. Commandeur, and N. P. E. Vermeulen.** 2006. Enantioselective substrate binding in a monooxygenase protein model by molecular dynamics and docking. Biophys. J. **91:**3206–3216.
16. **Felsenstein, J.** 2005. PHYLIP (Phylogeny Inference Package) version 3.6. Department of Genome Sciences, University of Washington, Seattle.
17. **Ferrández, A., B. Miñambres, B. García, E. R. Olivera, J. M. Luengo, J. L. García, and E. Díaz.** 1998. Catabolism of phenylacetic acid in *Escherichia coli*. Characterization of a new aerobic hybrid pathway. J. Biol. Chem. **273:**25974–25986.
18. **Gorlatov, S. N., O. V. Maltseva, V. I. Shevchenko, and L. A. Golovleva.** 1989. Degradation of chlorophenols by *Rhodococcus erythropolis*. Microbiology **58:**647–651.
19. **Higgins, D. G., and P. M. Sharp.** 1988. CLUSTAL: a package for performing multiple sequence alignment on a microcomputer. Gene **73:**237–244.
20. **Hollmann, F., K. Hofstetter, T. Habicher, B. Hauer, and A. Schmid.** 2005. Direct electrochemical regeneration of monooxygenase subunits for biocatalytic asymmetric epoxidation. J. Am. Chem. Soc. **127:**6540–6541.
21. **Hollmann, F., P.-C. Lin, B. Witholt, and A. Schmid.** 2003. Stereospecific biocatalytic epoxidation: the first example of direct regeneration of a FAD-dependent monooxygenase for catalysis. J. Am. Chem. Soc. **125:**8209–8217.
22. **Inoue, H., H. Nojima, and H. Okayama.** 1990. High efficiency transformation of *Escherichia coli* with plasmids. Gene **96:**23–28.
23. **Jones, J. B.** 2001. Biotransformations in organic chemistry. A textbook. Advanced synthesis & catalysis. Vol. 343, issue 6–7.
24. **Joosten, V., and W. J. H. van Berkel.** 2007. Flavoenzymes. Curr. Opin. Chem. Biol. **11:**195–202.
25. **Kantz, A., F. Chin, N. Nallamothu, T. Nguyen, and G. T. Gassner.** 2005. Mechanism of flavin transfer and oxygen activation by the two-component flavoenzyme styrene monooxygenase. Arch. Biochem. Biophys. **442:**102–116.
26. **Keil, H., C. M. Saint, and P. A. Williams.** 1987. Gene organization of the first catabolic operon of TOL plasmid pWW53: production of indigo by the *xylA* gene product. J. Bacteriol. **169:**764–770.
27. **Kende, A. S., P. Delair, and B. E. Blass.** 1994. A new paradigm for alkene epoxidation. Activation of hydrogen peroxide by organophosphorus electrophiles. Tetrahedron Lett. **35:**8123–8126.
28. **Kirchner, U., A. H. Westphal, R. Müller, and W. J. H. van Berkel.** 2003. Phenol hydroxylase from *Bacillus thermoglucosidasius* A7, a two-protein component monooxygenase with a dual role for FAD. J. Biol. Chem. **278:**47545–47553.
29. **König, C., D. Eulberg, J. Gröning, S. Lakner, V. Seibert, S. R. Kaschabek, and M. Schlömann.** 2004. A linear megaplasmid, p1CP, carrying the genes for chlorocatechol catabolism of *Rhodococcus opacus* 1CP. Microbiology **150:**3075–3087.
30. **Kuzmic, P.** 1996. Program DYNAFIT for the analysis of enzyme kinetic data: application to HIV proteinase. Anal. Biochem. **237:**260–273.
31. **Larkin, M. J., L. A. Kulakov, and C. C. R. Allen.** 2005. Biodegradation and *Rhodococcus*—masters of catabolic versatility. Curr. Opin. Biotechnol. **16:**282–290.
32. **Leonida, M. D.** 2001. Redox enzymes used in chiral syntheses coupled to coenzyme regeneration. Curr. Med. Chem. **8:**345–369.
33. **Li, Z., J. B. van Beilen, W. A. Duetz, A. Schmid, A. de Raadt, H. Griengl, and B. Witholt.** 2002. Oxidative biotransformations using oxygenases. Curr. Opin. Chem. Biol. **6:**136–144.
34. **Liu, L., R. D. Schmid, and V. B. Urlacher.** 2006. Cloning, expression, and characterization of a self-sufficient cytochrome P450 monooxygenase from *Rhodococcus ruber* DSM 44319. Appl. Microbiol. Biotechnol. **72:**876–882.
35. **Marchuk, D., M. Drumm, A. Saulino, and F. S. Collins.** 1991. Construction of T-vectors, a rapid and general system for direct cloning of unmodified PCR products. Nucleic Acids Res. **19:**1154.
36. **Massey, V.** 1994. Activation of molecular oxygen by flavins and flavoproteins. J. Biol. Chem. **269:**22459–22462.
37. **Moiseeva, O. V., I. P. Solyanikova, S. R. Kaschabek, J. Gröning, M. Thiel, L. A. Golovleva, and M. Schlömann.** 2002. A new modified ortho-cleavage pathway of 3-chlorocatechol degradation by *Rhodococcus opacus* 1CP: genetic and biochemical evidence. J. Bacteriol. **184:**5282–5292.
38. **Munro, A. W., D. G. Leys, K. J. McLean, K. R. Marshall, T. W. B. Ost, S. Daff, C. S. Miles, S. K. Chapman, D. A. Lysek, C. C. Moser, C. C. Page, and P. L. Dutton.** 2002. P450 BM3: the very model of a modern flavocytochrome. Trends Biochem. Sci. **27:**250–257.
39. **Munro, A. W., H. M. Girvan, and K. J. McLean.** 2007. Cytochrome P450—redox partner fusion enzymes. Biochim. Biophys. Acta **1770:**345–359.
40. **Narhi, L. O., and A. J. Fulco.** 1986. Characterization of a catalytically self-sufficient 119,000-dalton cytochrome P-450 monooxygenase induced by barbiturates in *Bacillus megaterium*. J. Biol. Chem. **261:**7160–7169.
41. **Ngai, K. L., M. Schlömann, H.-J. Knackmuss, and L. N. Ornston.** 1987. Dienelactone hydrolase from *Pseudomonas* sp. strain B13. J. Bacteriol. **169:**699–703.
42. **O'Connor, K. E., A. D. Dobson, and S. Hartmans.** 1997. Indigo formation by microorganisms expressing styrene monooxygenase activity. Appl. Environ. Microbiol. **63:**4287–4291.
43. **O'Leary, N. D., K. E. O'Connor, and A. D. W. Dobson.** 2002. Biochemistry, genetics and physiology of microbial styrene degradation. FEMS Microbiol. Rev. **26:**403–417.
44. **Otto, K., K. Hofstetter, M. Roethlisberger, B. Witholt, and A. Schmid.** 2004. Biochemical characterization of StyAB from *Pseudomonas* sp. strain VLB120 as a two-component flavin-diffusible monooxygenase. J. Bacteriol. **186:**5292–5302.
45. **Panke, S., M. Held, M. G. Wubbolts, B. Witholt, and A. Schmid.** 2002. Pilot-scale production of (S)-styrene oxide from styrene by recombinant *Escherichia coli* synthesizing styrene monooxygenase. Biotechnol. Bioeng. **80:**33–41.
46. **Parry, R. J., and W. Li.** 1997. An NADPH:FAD oxidoreductase from the valanimycin producer, *Streptomyces viridifaciens*. Cloning, analysis, and overexpression. J. Biol. Chem. **272:**23303–23311.
47. **Ramos, J. L., E. Duque, M.-T. Gallegos, P. Godoy, M. I. Ramos-González, A.**

Downloaded from jb.asm.org at Wageningen UR Library on August 23, 2009

Rojas, W. Terán, and A. Segura. 2002. Mechanisms of solvent tolerance in gram-negative bacteria. Annu. Rev. Microbiol. **56:**743–768.

48. **Roy, S.** 1999. Multifunctional enzymes and evolution of biosynthetic pathways: retro-evolution by jumps. Proteins **37:**303–309.
49. **Rudroff, F., V. Alphand, R. Furstoss, and M. D. Mihovilovic.** 2006. Optimizing fermentation conditions of recombinant *Escherichia coli* expressing cyclopentanone monooxygenase. Org. Process Res. Dev. **10:**599–604.
50. **Sambrook, J., E. Fritsch, and T. Maniatis.** 2001. Molecular cloning: a laboratory manual, 3rd ed. Cold Spring Harbor Laboratory Press, Cold Spring Harbor, NY.
51. **Schmid, A., K. Hofstetter, H.-J. Feiten, F. Hollmann, and B. Witholt.** 2001. Integrated biocatalytic synthesis on gram scale: the highly enantioselective preparation of chiral oxiranes with styrene monooxygenase. Adv. Synth. Catal. **343:**732–737.
52. **Siu, E., K. Won, and C. Park.** 2007. Electrochemical regeneration of NADH using conductive vanadia-silica xerogels. Biotechnol. Prog. **23:**293–296.
53. **Testa, B., and P. Jenner.** 1981. Inhibitors of cytochrome P-450s and their mechanism of action. Drug Metab. Rev. **12:**1–117.
54. **Thiel, M., S. R. Kaschabek, J. Gröning, M. Mau, and M. Schlömann.** 2005. Two unusual chlorocatechol catabolic gene clusters in *Sphingomonas* sp. TFD44. Arch. Microbiol. **183:**80–94.
55. **Thompson, J. D., T. J. Gibson, F. Plewniak, F. Jeanmougin, and D. G. Higgins.** 1997. The CLUSTAL_X windows interface: flexible strategies for multiple sequence alignment aided by quality analysis tools. Nucleic Acids Res. **25:**4876–4882.
56. **Torres Pazmiño, D. E., R. Snajdrova, B.-J. Baas, M. Ghobrial, M. D. Mihovilovic, and M. W. Fraaije.** 2008. Self-sufficient Baeyer-Villiger monooxygenases: effective coenzyme regeneration for biooxygenation by fusion engineering. Angew. Chem. Int. Ed. **47:**2275–2278.
57. **van Berkel, W. J. H., N. M. Kamerbeek, and M. W. Fraaije.** 2006. Flavoprotein monooxygenases, a diverse class of oxidative biocatalysts. J. Biotechnol. **124:**670–689.
58. **van den Heuvel, R. H. H., A. H. Westphal, A. J. R. Heck, M. A. Walsh, S. Rovida, W. J. H. van Berkel, and A. Mattevi.** 2004. Structural studies on flavin reductase PheA2 reveal binding of NAD in an unusual folded conformation and support novel mechanism of action. J. Biol. Chem. **279:**12860–12867.
59. **van der Geize, R., and L. Dijkhuizen.** 2004. Harnessing the catabolic diversity of rhodococci for environmental and biotechnological applications. Curr. Opin. Microbiol. **7:**255–261.
60. **van Hellemond, E. W., D. B. Janssen, and M. W. Fraaije.** 2007. Discovery of a novel styrene monooxygenase originating from the metagenome. Appl. Environ. Microbiol. **73:**5832–5839.
61. **van Hellemond, E. W., M. van Dijk, D. P. H. M. Heuts, D. B. Janssen, and M. W. Fraaije.** 2008. Discovery and characterization of a putrescine oxidase from *Rhodococcus erythropolis* NCIMB 11540. Appl. Microbiol. Biotechnol. **78:**455–463.

Downloaded from jb.asm.org at Wageningen UR Library on August 23, 2009